DEVELOPMENTAL BIOLOGY

# *Insm1*-expressing neurons and secretory cells develop from a common pool of progenitors in the sea anemone *Nematostella vectensis*

**Océane Tournière[1], James M. Gahan[1]†, Henriette Busengdal[1]†, Natascha Bartsch[1,2], Fabian Rentzsch[1,2]***



**Neurons are highly specialized cells present in nearly all animals, but their evolutionary origin and relationship to other cell types are not well understood. We use here the sea anemone *Nematostella vectensis* as a model system for early-branching animals to gain fresh insights into the evolutionary history of neurons. We generated a transgenic reporter line to show that the transcription factor *NvInsm1* is expressed in postmitotic cells that give rise to various types of neurons and secretory cells. Expression analyses, double transgenics, and gene knockdown experiments show that the *NvInsm1*-expressing neurons and secretory cells derive from a common pool of *NvSoxB(2)*-positive progenitor cells. These findings, together with the requirement for *Insm1* for the development of neurons and endocrine cells in vertebrates, support a close evolutionary relationship of neurons and secretory cells.**

## INTRODUCTION

Neurons are cells with a high diversity of morphological, molecular, and physiological properties. The common theme of neurons is the presence of subcellular structures that allow fast and precise intercellular communication. Many neurons have long processes, collectively termed neurites, that are used for the propagation of electrical excitation. These electrical signals trigger the release of the content of small vesicles either in a highly specific manner at chemical synapses or with lower temporal and spatial resolution via neurosecretion. The sophisticated molecular machineries that enable electrical conductance and vesicle release resemble those found in other cell types. The electrical excitability and conduction in muscle cells are based on the same types of voltage-gated sodium and calcium channels as that of neurons, whereas the release of synaptic vesicles involves many proteins associated with the vesicle and plasma membrane, respectively, that also function in vesicle release from non-neural secretory and endocrine cells. The evolution of neurons thus likely resulted from the elaboration of different preexisting cellular modules (*1*–*7*). Since the presence of the constituents of these different cellular modules within the same cell requires their coordinated expression, analyzing the gene regulatory program and the developmental origin of neurons in different species can provide valuable insights into the evolutionary relationship between neurons and other cell types. Here, we follow this approach by addressing the development of neurons and gland/secretory cells in the sea anemone *Nematostella vectensis*, a member of an animal clade that separated from the bilaterian lineage (e.g., chordates, arthropods, nematodes, and annelids) more than 600 million years ago (*8*, *9*).

Vertebrate neurons originate from the ectoderm, whereas endocrine cells of the gastrointestinal system originate from the endoderm. Despite this substantial difference, there are many similarities in the development of neurons and endocrine cells. They involve the use of conserved signaling molecules and transcription factors like Notch signaling, soxB genes, and bHLH genes of the atonal, neurogenin, and achaete-scute families (*10*–*12*). For example, inactivation of Notch signaling in mice results in a neurogenic phenotype characterized by an excess of neurons (*13*, *14*) and in the development of excess endocrine cells in the pancreas (*15*). Similarly, transcription factors of the neurogenin family are required for the development of olfactory sensory neurons (*16*) and for the formation of endocrine cells in the gastrointestinal tract (*17*–*19*). Interpretations of these similarities are confounded, however, by the use of different paralogs in different cell types and tissues, e.g., *neurogenin1* in the olfactory epithelium and *neurogenin3* in the gastrointestinal tract, and by the widespread functions of some of these gene families in the specification of other cell types [e.g., (*20*, *21*)].

A more notable case is the zinc finger transcription factor Insulinoma-associated protein 1 (Insm1 or IA-1). During mouse embryonic development, *Insm1* is expressed broadly in the central and peripheral nervous system, in the stomach, intestine, pancreas, thymus, thyroid, and adrenal glands (*22*–*25*). Analyses of knockout mice revealed that *Insm1* is required for the development of neurons throughout the brain (*26*, *27*) and of neural crest–derived cells of the sympathoadrenal lineage in the peripheral nervous system (*28*). Moreover, *Insm1* controls the development of endocrine cells in the pancreas, lung, intestine, and pituitary gland (*22*, *23*, *29*, *30*). The broad roles of *Insm1* in the development of neurons and endocrine cells make it a particularly interesting candidate gene for addressing the evolutionary relationship between neural and secretory cells.

Cnidarians (e.g., sea anemones, corals, and jellyfish) are the sister taxon to bilaterians (*31*, *32*) and the earliest-branching group of animals whose nervous system unambiguously shares a common origin with that of bilaterians (*33*). There are two major groups of cnidarians, anthozoans and medusozoans, with the polyp as the body form common to both groups and the medusa as a pelagic life cycle stage present only in medusozoans. Polyps can be described as a tube with one opening, which is surrounded by tentacles used for the capture of prey (*34*). Notwithstanding local differences in the density of neurons and neurites, the nervous system of cnidarian polyps is best described as a nerve net that lacks brain-like centralization.

[1]Sars International Centre for Marine Molecular Biology, University of Bergen, 5006 Bergen, Norway. [2]Department of Biological Sciences, University of Bergen, 5006 Bergen, Norway.
*Corresponding author. Email: fabian.rentzsch@uib.no
†These authors contributed equally to this work.

Three general classes of neural cells are distinguished in cnidarians: sensory/sensory-motor neurons, ganglion cells (potentially equivalent to interneurons), and cnidocytes, the cnidarian-specific stinging cells (*35*–*37*). The developmental origin of neural cells appears to differ between different groups of cnidarians. In hydrozoans (a subgroup of medusozoans), the so-called interstitial stem cells give rise to neural cells. The interstitial stem cell population also gives rise to gland/secretory cells and gametes, but similar nonepithelial stem cells have not been observed outside this particular group of cnidarians (*37*–*40*). The molecular control of neurogenesis in cnidarians is currently best understood in the anthozoan *N. vectensis* (*35*, *41*), in which soxB genes, Notch signaling, and bHLH genes of the atonal/neurogenin and achaete-scute families regulate the development of neural cells (*42*–*46*). In particular, a pool of epithelial *NvSoxB(2)*-expressing progenitor cells has been identified that gives rise to sensory neurons, ganglion cells, and cnidocytes during embryonic development (*44*). Inhibition of *NvSoxB(2)* or *NvAtonal-like* (*NvAth-like*) resulted in a strong reduction in the number of neurons and cnidocytes, whereas inhibition of Notch signaling increased their numbers (*43*–*45*). These observations identified a substantial degree of similarity in the genetic programs regulating the early stages of *Nematostella* and vertebrate neurogenesis. In contrast to vertebrates, however, neurogenesis in *Nematostella* occurs both in the ectoderm and in the mesendoderm, the only two germ layers in the diploblastic cnidarians (*44*, *47*). The development of gland/secretory cells is not well understood in *Nematostella*, but it has recently been shown that gland/secretory cells expressing either digestive enzymes or insulin-like peptides are located in tissues of ectodermal origin. These tissues are the ectodermal part of the pharynx and the septal filaments, which are extensions of the pharyngeal ectoderm (*48*). The septal filaments extend along the oral-aboral axis of the animals and are part of internal structures of anthozoans called mesenteries (Fig. 1A). The ectodermal origin of these gland/secretory cells is in contrast to the endodermal origin of equivalent cells in the vertebrate midgut and pancreas (*48*).

To better understand the relationship between neurons and gland/secretory cells, we studied here the role of *NvInsm1* in *Nematostella*. We generated transgenic reporter lines to show that *NvInsm1*-expressing cells give rise to a large number of sensory and ganglion cells, but not to cnidocytes. We further show that *NvInsm1*::GFP-positive cells coexpress *NvTrypsin*, *NvInsulin-like peptide* (*NvIlp*), and *NvMucin* in different populations of gland/secretory cells in the pharyngeal and body wall ectoderm, and that the expression of these genes is reduced upon knockdown of *NvInsm1*. Using double transgenics, we observe that *NvSoxB(2)*-expressing cells give rise not only to neurons but also to *NvInsm1*::GFP-positive gland/secretory cells, and we find that knockdown of *NvSoxB(2)* results in the down-regulation of *NvInsm1* and gland/secretory cell genes. Our data show that neurons and gland/secretory cells in *Nematostella* originate from a common pool of progenitor cells and that their development involves *NvInsm1*. These findings support the hypothesis that neurons and secretory cells share a common evolutionary origin.

## RESULTS

### *NvInsm1* is expressed in nonproliferating, differentiating neural cells

The *Nematostella* genome encodes a single Insm1 ortholog (*NvInsm1*) with six C2H2 Zn-finger domains and a SNAG domain at the N terminus (fig. S1A). The domain composition of NvINSM1 is more similar to human and mouse INSM1 (five Zn-fingers and a SNAG domain) than the *Drosophila melanogaster* and *Caenorhabditis elegans* orthologs, which each has three Zn-fingers and lacks the SNAG domain (fig. S1, A and B), which is required for interaction with chromatin-modifying proteins (*29*, *49*, *50*). Phylogenetic analysis based on the first three Zn-finger domains confirmed the assignment of NvINSM1 as an Insm1 ortholog (fig. S1C). By in situ hybridization (ISH), the expression of *NvInsm1* starts at the mid-blastula stage in few scattered cells in the epithelium (Fig. 1, B and C). At the late blastula and early gastrula stages, the number of *NvInsm1*-expressing cells increases and is restricted to the aboral half of the embryo (Fig. 1, D, E, and I). At the late gastrula stage, cells at the oral side also initiate expression (Fig. 1, F and J). *NvInsm1* starts being expressed in many pharyngeal cells at the early planula stage (Fig. 1, G and K), and by the late planula stage, it can be detected in mesendodermal single cells (Fig. 1, H and L). To test whether *NvInsm1* is expressed in proliferating cells, we exposed wild-type animals at the planula stage to the thymidine analog 5-ethynyl-2′-deoxyuridine (EdU), fixed, and performed EdU detection together with immunostaining using an antibody raised against NvINSM1 (Fig. 1, M to P, and fig. S2J). After a 30-min EdU pulse, we could not detect cells expressing NvINSM1 and incorporating EdU. After 2 and 4 hours of EdU pulse, we could observe a very small number of NvINSM1$^+$ cells incorporating EdU (0.56 and 2.27%, respectively) (Fig. 1, O and P). EdU pulse labeling in combination with fluorescence ISH (FISH) likewise did not reveal proliferating *NvInsm1*-expressing cells (fig. S3). This suggests that *NvInsm1* is mostly expressed in nonproliferating cells.

To characterize the nature of the *NvInsm1*-expressing cells further, we generated stable transgenic reporter lines, *NvInsm1*::*GFP* and *NvInsm1*::*mCherry*, in which a 4.6-kb region upstream of the open reading frame of *NvInsm1* drives the expression of a membrane-tethered GFP (or membrane-tethered mCherry). This allows the identification of the *NvInsm1*-expressing cells and their progeny during development. Double FISH of *GFP* and *NvInsm1* on transgenic embryos showed a high degree of coexpression of the reporter gene transcripts and endogenous *NvInsm1* (fig. S4), confirming that the reporter lines reflect the endogenous expression of *NvInsm1*.

Analysis of the *NvInsm1*::*GFP* line reveals that the transgene is expressed from the early gastrula stage in scattered ectodermal cells. At this stage, the cells are elongated along the apical-basal axis, with some having a cilium and others having microvilli-like protrusions on their apical surface (Fig. 2, A and B). At the planula stage, many of the GFP$^+$ ectodermal cells form neurites with varicosities on their basal side (Fig. 2, C and D). At the primary polyp stage, GFP labels the ectodermal and mesendodermal nerve net of the animal (Fig. 2, E to G). At this stage, there is also GFP expression in many cells of the pharynx and in the ectodermal parts of the two primary mesenteries (the septal filaments; Fig. 2, H to M). Most GFP$^+$ cells in the pharynx are elongated along their apical-basal axis and have a cilium on the apical membrane (Fig. 2I), while some cells are not elongated and seem to contain many vesicle-like structures labeled by the membrane-tethered GFP (Fig. 2J). Among the vesicle-filled cells, we observe some that also carry an apical cilium (Fig. 2M). The *NvInsm1*::*GFP* reporter line thus labels cells with different morphologies, including cells of neuronal appearance.

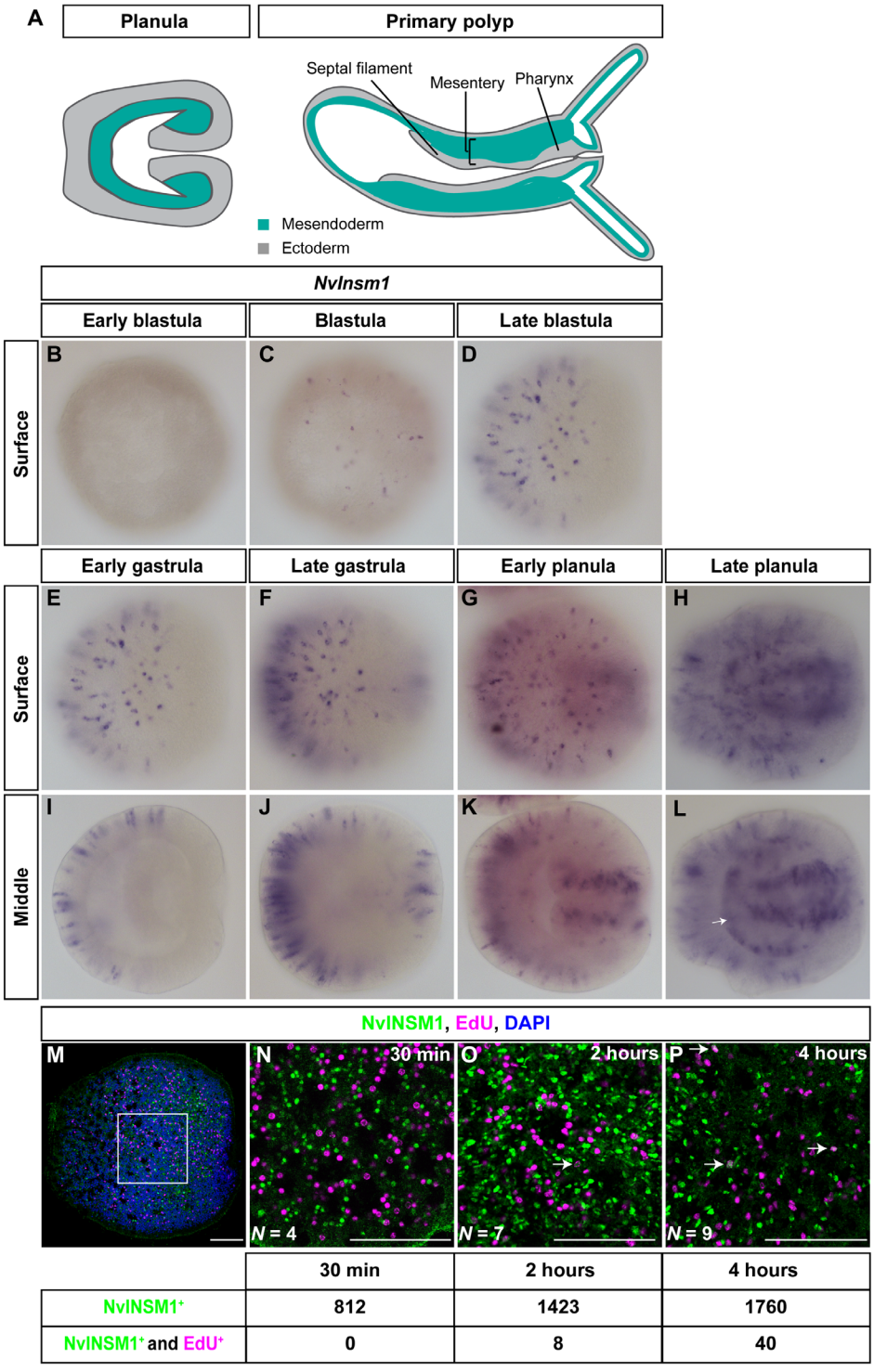


| | 30 min | 2 hours | 4 hours |
|---|---|---|---|
| NvINSM1$^+$ | 812 | 1423 | 1760 |
| NvINSM1$^+$ and EdU$^+$ | 0 | 8 | 40 |

**Fig. 1. *NvInsm1* is expressed in scattered postmitotic cells.** (**A**) Cartoons of *Nematostella* at the planula and primary polyp stages. Tissues of mesendodermal and ectodermal origin are labeled in green and gray, respectively. Aboral pole to the left, drawings are not to scale. (**B** to **L**) *NvInsm1* ISH with the developmental stage indicated on the top. Mid-lateral views with the aboral pole to the left. (B) to (H) are focused on the surface of the specimens, and (I) to (L) are optical sections at the middle of the specimens. Starting at blastula stage (12 hpf), *NvInsm1* is expressed in scattered single cells, mainly in the aboral half of the embryos. At the early planula stage, *NvInsm1* starts being expressed in the forming pharynx (K). At the late planula stage (L), *NvInsm1* starts being expressed in the mesendoderm, indicated by the white arrow. (**M** to **P**) Immunostaining of NvINSM1 (green), 5-ethynyl-2′-deoxyuridine (EdU) (magenta), and 4′,6-diamidino-2-phenylindole (DAPI) (blue) at the planula stages. Staining is indicated at the top. (N) None of the ectodermal cells expressing NvINSM1 incorporated EdU after a 30-min pulse. After 2 hours (O) and 4 hours (P) of EdU exposure, some EdU$^+$/NvINSM1$^+$ cells can be detected [white arrows in (O) and (P)]. *N* stands for the number of embryos analyzed. Scale bars, 20 μm.

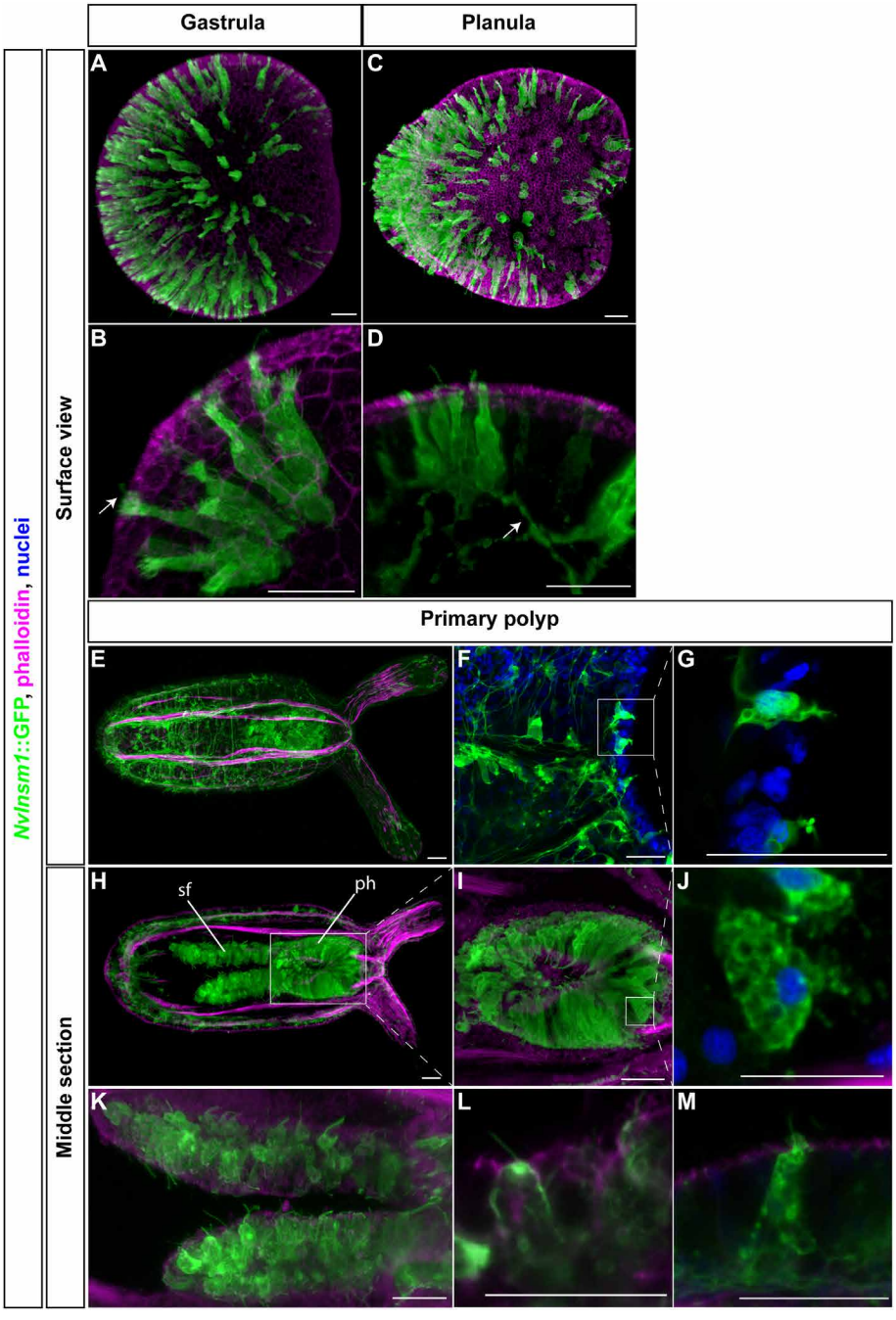


**Fig. 2. A *NvInsm1* transgenic reporter identifies morphologically diverse cell types.** (**A** to **M**) In confocal microscopy images of the *NvInsm1*::GFP transgenic line, GFP is detected by anti-GFP antibody (green), F-actin by phalloidin (magenta), and DNA by DAPI (blue), except (F) and (G), which show live imaging of GFP (green) and Hoechst (blue). Developmental stages are indicated on the top, the focal plane (surface or middle) is indicated on the left side. All images are lateral views with the aboral pole to the left. The white arrow in (B) points toward a cell surface with microvilli-like protrusions. The white arrow in (D) shows the forming neurites. (I) is a higher magnification of the area indicated in (H), and (G) and (J) are higher magnifications of the boxed areas in (F) and (J), respectively. All images are Imaris snapshots from three-dimensional (3D) reconstructions, except images (G), (J), (L), and (M), which are stacks (two to three confocal sections) generated with Fiji. Pictures (F and G) were taken from live animals (see Material and Methods). Expression of GFP is detected from the gastrula stage and is consistent with the ISH signals (fig. S2). ph, pharynx; sf, septal filament. Scale bars, 20 μm.

### *NvInsm1*-expressing cells give rise to sensory and ganglion neurons

To better characterize the identity of the *NvInsm1*-expressing cells, we used double FISH to test the coexpression of *NvInsm1* with the neuropeptide gene *NvRFamide* [labeling a subset of differentiating sensory and ganglion cells) (Fig. 3, A to H) (*51*). We observed that *NvInsm1* and *NvRFamide* are partially co-expressed in the ectoderm from the blastula to the planula stage (Fig. 3, A to F) and in the developing pharynx at the planula stage (Fig. 3, G and H).

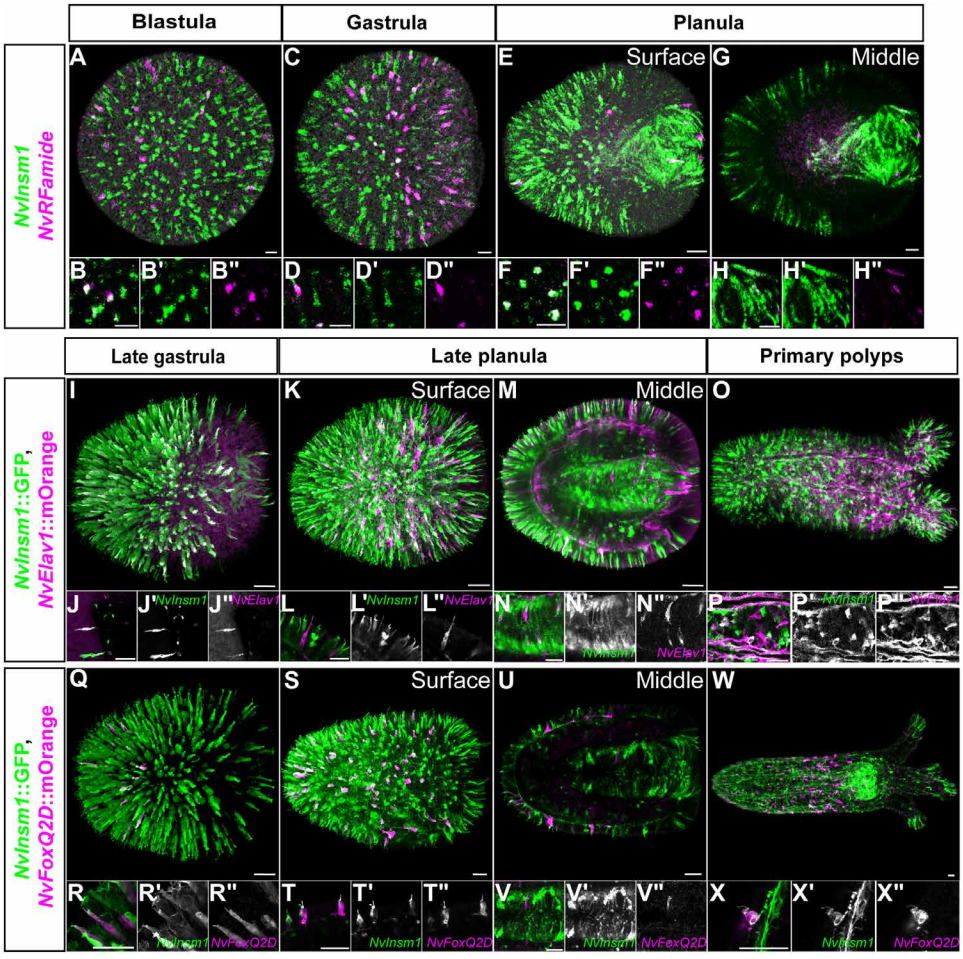


**Fig. 3. *NvInsm1*-expressing cells give rise to sensory and ganglion cells.** Developmental stages are indicated at the top, and the labeling is indicated on the left. (**A** to **H**) Double FISH for *NvInsm1* (green) and the neuronal differentiating marker *NvRFamide* (magenta) show coexpression from the blastula stage to the planula stage. (B), (D), and (F) are higher magnifications of ectodermal regions at the blastula, gastrula, and planula, respectively. (H) is a higher magnification of the pharynx. (**I** to **P**) Double transgenic animals with *NvInsm1*::GFP (green) and *NvElav1*::mOrange (magenta). Almost all *NvElav1*::mOrange$^+$ cells are GFP$^+$. (**Q** to **X**) Double transgenic animals with *NvInsm1*::GFP (green) and *NvFoxQ2d*::mOrange (magenta). From gastrula to primary polyps, most of the *NvFoxQ2d*::mOrange$^+$ cells are also GFP$^+$. (J), (L), (R), (T), and (X) show higher magnifications of ectodermal cells; (N) and (M) identify coexpression in the pharynx; and (P) shows coexpression in mesendodermal neurons in the body column. All pictures are lateral views with aboral pole to the left. (A), (C), (E), (I), (K), (O), (Q), (S), and (W) are Imaris snapshots from three-dimensional (3D) reconstructions to show overviews. All other pictures are stacks of two to three confocal sections to confirm coexpression of the signals. Scale bars, 20 μm.

Next, we generated double transgenic animals by crossing *NvInsm1*::GFP animals with previously characterized transgenic reporter lines. The *NvElav1*::*mOrange* transgenic line labels a large fraction of sensory and ganglion cells but not cnidocytes (*47*). At late gastrula, all *NvElav1*::mOrange$^+$ cells are also *NvInsm1*::GFP$^+$, suggesting that a subset of the *NvInsm1*-expressing cells are sensory and ganglion cells (Fig. 3, I and J). From the late planula to the primary polyp stage, most of the *NvElav1*::mOrange$^+$ cells are still expressing the GFP transgene, including cells present in the pharynx and in the forming tentacles (Fig. 3, K to P).

The *NvFoxQ2d*::*mOrange* line labels a small population of ectodermal sensory cells, which does not coexpress *NvElav1*::cerulean (*52*). In double transgenics, we identified the *NvFoxQ2d*::mOrange$^+$ cells as a subpopulation of the *NvInsm1*::GFP$^+$ cells (Fig. 3, Q to X). These observations were also confirmed by studying the presence of NvINSM1 protein in those transgenic lines (fig. S2, A to I). Thus, the *NvInsm1* transgenic reporter line identifies two of the main classes of neurons in *Nematostella*, sensory cells and ganglion cells.

### *NvInsm1*-expressing cells do not give rise to cnidocytes

We next analyzed whether *NvInsm1*-expressing cells also give rise to the third class of cnidarian neural cells, the cnidocytes. First, we studied *NvInsm1* expression with *NvNcol3* (a gene expressed in differentiating cnidocytes) via double FISH (fig. S5, A to H). The two transcripts do not colocalize from the blastula to the planula stage, but we cannot discard the possibility that they are expressed sequentially in the same cells. To investigate this hypothesis, we generated double transgenics with the *NvNcol3*::*mOrange2* line, which identifies differentiating and mature cnidocytes (*53*). The two transgenes are not coexpressed from the onset of the *NvNcol3*::mOrange2 expression at the late gastrula stage to the primary polyp stage (fig. S5, I to P). On the basis of these two analyses, we conclude

that *NvInsm1*-expressing cells do not contribute to the formation of cnidocytes.

### Some *NvInsm1*-expressing cells develop into gland/secretory cells

From the planula to the primary polyp stage, the number of *NvInsm1*-expressing cells in the developing pharynx and in the septal filaments along the mesenteries seems to increase. These two structures contain many neural cells, but they have also been described to contain many gland/secretory cells expressing genes encoding digestive enzymes or genes related to mucus secretion (*48*). To test whether *NvInsm1*-expressing cells contribute to populations of gland/secretory cells, we performed FISH in the background of the *NvInsm1::GFP* line at the planula stage (Fig. 4, A to F). We observed that *NvInsm1*::GFP is coexpressed with *NvMucin* in putative mucous cells of the ectoderm of the body column and in the forming pharynx (Fig. 4, A and B) (*48*). We also observed coexpression in the pharynx with *NvTrypsinA* (expressed in putative gland cells with digestive function; Fig. 4, C and D) and with insulin-like peptide 3 (*NvILP3*; Fig. 4, E and F) (*48*). Analysis of the published *Nematostella* single-cell sequencing data (*54*) supported our morphological observation by identifying *NvInsm1* as enriched in 1 of 13 larval metacells designated as "progenitors/undifferentiated," in 3 of 6 "neuronal," and in 3 of 4 "gland/secretory" larval metacells (fig. S6, A and B). We conclude that a subpopulation of the *NvInsm1*-expressing cells gives rise to different types of gland/secretory cells in *Nematostella*.

To understand whether this expression profile is conserved in other cnidarians, we used the single-cell RNA sequencing analysis performed in *Hydra* (*55*), a distantly related cnidarian species. The *Hydra* genome encodes a single *Insm1-like* gene that contains two C2H2 zinc fingers (and was therefore not included in our phylogenetic analysis) that show strong similarity to Insm1 proteins from other species. *HvInsm1-like* appears to be present in ectodermal and endodermal neurons as well as in gland/secretory cells and in their progenitors (fig. S7). As in *Nematostella*, *HvInsm1-like* is not expressed in differentiated cnidocytes and in nematoblasts (cnidocyte progenitors). Together, these data suggest that, in cnidarians, *Insm1* is expressed in sensory and ganglion cells as well as in gland/secretory cells.

### Knockdown of *NvInsm1* reduces the expression of marker genes for gland/secretory cells

To test the function of *NvInsm1*, we used a short hairpin RNA (shRNA)–based knockdown approach (*56*). We injected two different shRNAs, which each led to an approximately 2.6-fold down-regulation of *NvInsm1* transcripts without affecting the overall morphology at the planula stage (Fig. 5, A to D). Quantitative reverse transcription polymerase chain reaction (qRT-PCR) showed that the expression levels of the gland/secretory cell genes *NvILP3*, *NvMucin*, and *NvTrypsinA* were significantly down-regulated (Fig. 5D), and ISH revealed that the number of cells expressing these genes is reduced (Fig. 5, E to L). This shows that *NvInsm1* is required for the gene expression program of at least some gland/secretory cells. In contrast, the expression levels of the neuron-specific genes *NvElav1*, *NvFoxQ2d*, and *NvRFamide* were not significantly different from animals injected with a control shRNA (Fig. 5D). These data suggest that either the level of *NvInsm1* knockdown was not sufficient to affect neural gene expression or *NvInsm1* is not required for the expression of the analyzed neural genes.

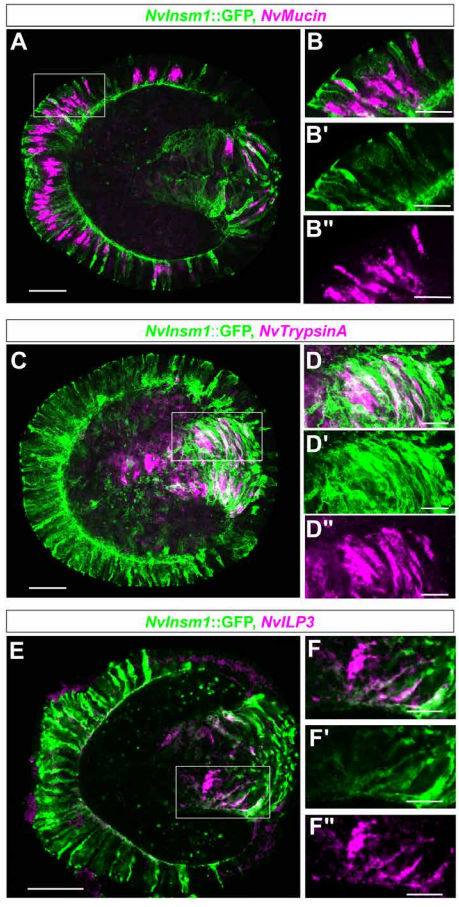


**Fig. 4. Gland/secretory cells derive from *NvInsm1*::GFP-expressing cells.** (**A** to **F**) Confocal images of fluorescence ISHs in *NvInsm1*::GFP transgenic planulae. GFP (green) is detected by immunohistochemistry, and in situ probes are indicated on the top and shown in magenta. (B), (D), and (F) are higher magnifications of the boxed areas in (A), (C), and (E), respectively. Lateral views with the aboral pole to the left. Transcripts for *NvMucin*, *NvTrypsinA*, and *NvILP3* are detected in *NvInsm1*::GFP-positive cells. All pictures are stacks of one to three confocal sections. Scale bars, 50 μm (A, C, and E) and 20 μm (B, D, and F).

### The *NvSoxB(2)*-expressing progenitor cell population gives rise to neural and gland/secretory cells

During *Nematostella* embryogenesis, a *NvSoxB(2)*-expressing population of cells gives rise to sensory cells, ganglion cells, and cnidocytes (*44*). Comparison of ISH at different developmental stages (fig. S8, A to N) showed that the expression of *NvSoxB(2)* in the blastoderm commences earlier than that of *NvInsm1* (fig. S8, A, B, I, and H) and that, similarly, expression of *NvSoxB(2)* in the pharynx and the mesendoderm precedes that of *NvInsm1* (fig. S8, E, F, L, and M). In double FISHs (Fig. 6, A to H), we observed many cells co-expressing the two transcripts at the blastula, gastrula, and planula stages, but we also found cells expressing only one of the two genes. This is compatible with at least two not mutually exclusive scenarios: Individual cells might first express *NvSoxB(2)*, then coexpress *NvSoxB(2)* and *NvInsm1*, and eventually maintain only the expression of *NvInsm1*. Alternatively, the double-positive and single-positive cells might constitute different populations with different developmental potentials. To test these hypotheses, we generated *NvSoxB(2)*::mOrange, *NvInsm1*::GFP double transgenic animals

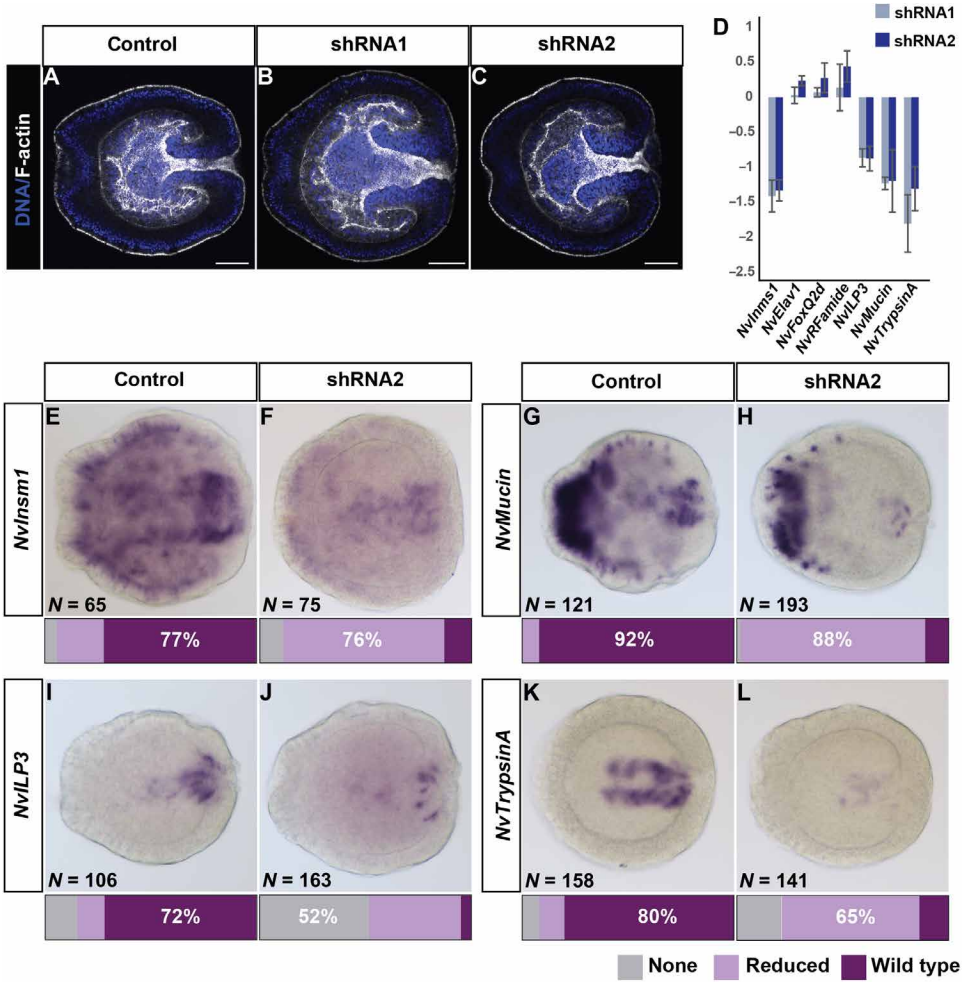


**Fig. 5. *NvInsm1* is required for the development of gland/secretory cells.** (**A** to **C**) Confocal images of planula injected with control shRNA (A), *NvInsm1* shRNA1 (B), or *NvInsm1* shRNA2 (C) stained for F-actin (gray) and DNA (blue). Lateral views with aboral pole to the left. (**D**) qRT-PCR on selected neural and gland/secretory cell genes at the planula stage after *NvInsm1* shRNA injection. Graphs show the mean ± SD of the log(2) fold change in expression between control shRNA and either NvInsm1 shRNA1 (light blue) or *NvInsm1* shRNA2 (dark blue) across three independent biological replicates. (**E** to **L**) Lateral views of ISHs at the planula stage with aboral pole to the left. Probes are indicated on the left, and injected shRNAs are indicated on the top. Expression of *NvInsm1* and three genes expressed in gland/secretory cells is reduced after injection of shRNA against *NvInsm1*. Bars at the bottom of each image represent the percentage of animals in each phenotypic class. *N* is the total from three biological replicates. Scale bars, 50 μm.

(Fig. 6, I to Z). At the gastrula, planula, and primary polyp stages, all detectable *NvInsm1*::GFP$^+$ cells were also labeled with the *NvSoxB(2)* reporter (Fig. 6, J, M, N, P, S, and T), but there were some *NvSoxB(2)*::mOrange$^+$ cells that were not GFP$^+$, suggesting that the developmental potential of *NvSoxB(2)*-expressing cells is broader than that of the *NvInsm1*$^+$ ones (Fig. 6, K and Q). If all *NvInsm1*::GFP$^+$ cells are part of the *NvSoxB(2)* lineage, then we would expect to find gland/secretory cells among the *NvSoxB(2)*::mOrange cells. This was indeed the case, as we identified double transgenic ectodermal cells containing vesicle-like structures (Fig. 6, X to Z, and fig. S9). This suggest that *NvSoxB(2)*-expressing cells constitute a population of progenitor cells that gives rise to neural cells and gland/secretory cells.

To test whether *NvSoxB(2)* function is required for the expression of *NvInsm1* and for the development of gland cells, we inhibited *NvSoxB(2)* by injection of a morpholino (MO) antisense oligonucleotide (*44*). This resulted in a nearly complete suppression of *NvInsm1* expression (Fig. 7, A and B) and a strong reduction in the number of *NvInsm1*::mCherry-expressing cells (Fig. 7, C to F). Furthermore, the number of cells expressing *NvMucin* (in pharynx and body wall ectoderm), *NvTrypsinA*, and *NvILP3* (both in the pharynx) was strongly reduced upon injection of *NvSoxB(2)* morpholinos (Fig. 7, I to N). Expression of *NvFoxA* showed that the pharynx is present in the injected animals but that it has a less elongated morphology (Fig. 7, O and P). Whether the perturbed formation of gland cells contributes to this altered morphology or, conversely, the altered morphology contributes to the reduced number of cells expressing gland cell markers remains unclear. The data suggest, however, that the effect of *NvSoxB(2)* MO injection on pharyngeal cells is unlikely to be due solely to a general effect on pharynx development.

Notch signaling and bHLH genes have been shown to affect neurogenesis in *Nematostella* (*43*, *45*, *57*), and we therefore addressed their potential involvement in regulating the expression of *NvInsm1*

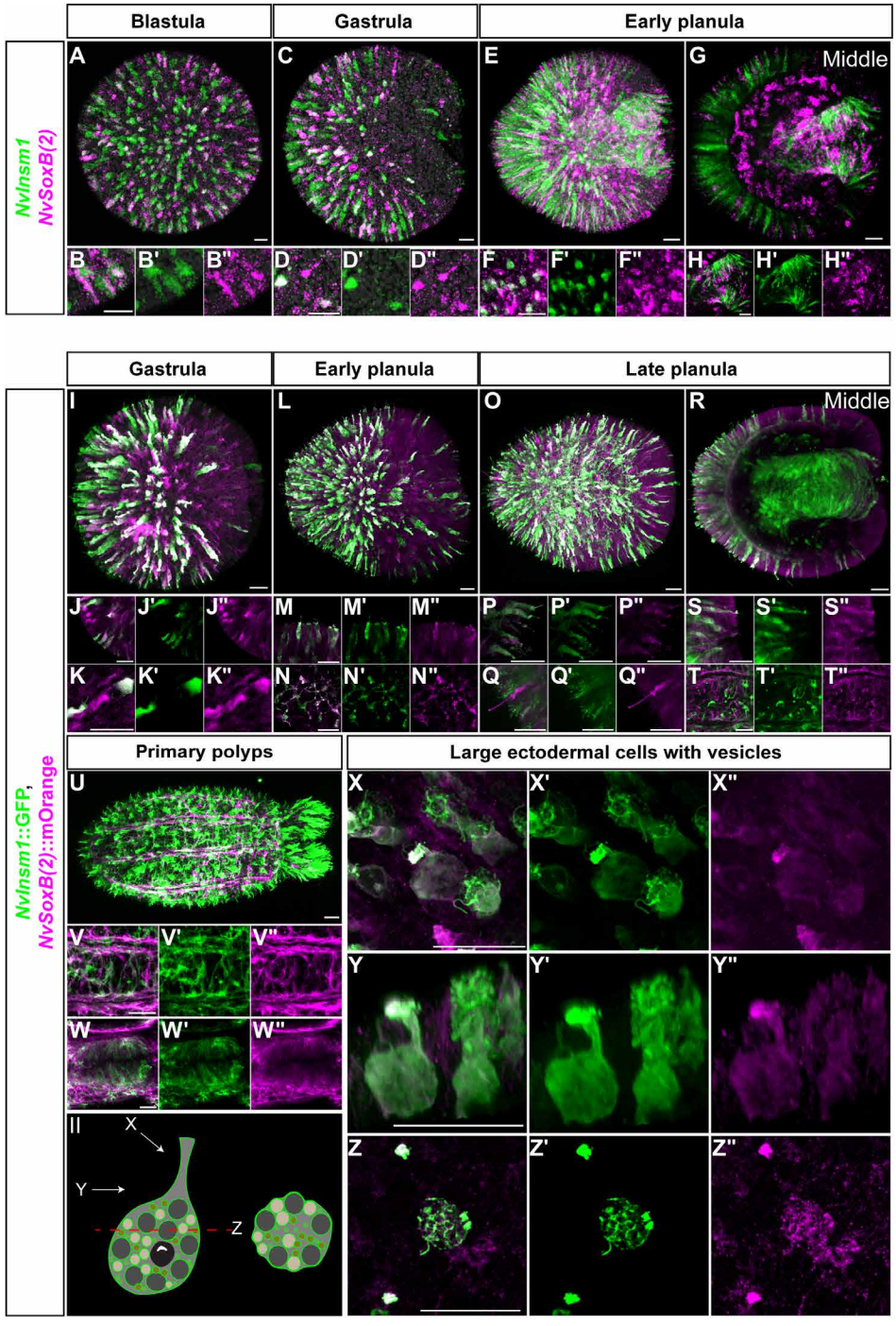


**Fig. 6. *NvInsm1*-expressing cells are generated from *NvSoxB(2)*-positive progenitors.** For (**A**) to (**Z**), probes or transgenes are represented on the left, and stages at the top. (A to H) Double FISH at the blastula stage for *NvInsm1* (green) and *NvSoxB(2)* (magenta) shows coexpression from the blastula to the early planula stage in ectodermal cells (A to F) and in the pharyngeal cells at early planula (G and H). All ISHs were performed with at least three replicates. Overview images (A, C, and E) are Imaris snapshots from 3D reconstructions. All other pictures are Fiji stacks of two confocal sections to confirm coexpression of the signals. (I to Z) Double transgenic animals with *NvInsm1*::GFP (green) and *NvSoxB(2)*:: mOrange (magenta). Lateral view with aboral pole to the left. From the gastrula to primary polyp stage, all *NvInsm1*::GFP$^+$ cells are also mOrange$^+$. (J), (M), (S), and (T) show snapshots of cells at different stages expressing both transgenes, and forming neurites are visible in (N). (V) Snapshot of the developing mesendodermal nerve net. (W) Snapshot of the developing pharynx at the primary polyp stage. At every stage, some large cells containing many vesicle-like structures also express both transgenes (X, Y, and Z). (II) Diagram representation of one of these cells with the different views taken in the (X) to (Z). (X) Surface view of these cells from a slightly oblique angle. **(**Y) Lateral view, 3D reconstruction of one cell. (Z) Single confocal cross section of one of the cells in the plane of the epithelium shows the vesicle-like structures. Some *NvSoxB(2)*::mOrange$^+$ cells are not GFP$^+$ (K and Q), suggesting that *NvInsm1* identifies a subset of the *NvSoxB(2)*-expressing cell population. (I), (L), (O), (U), (X), and (Y) are Imaris snapshots from the 3D reconstruction to show the overview staining. All other pictures [except (Z)] are Fiji stacks of two to three confocal sections to confirm the coexpression of the signals. Scale bar, 20 μm.

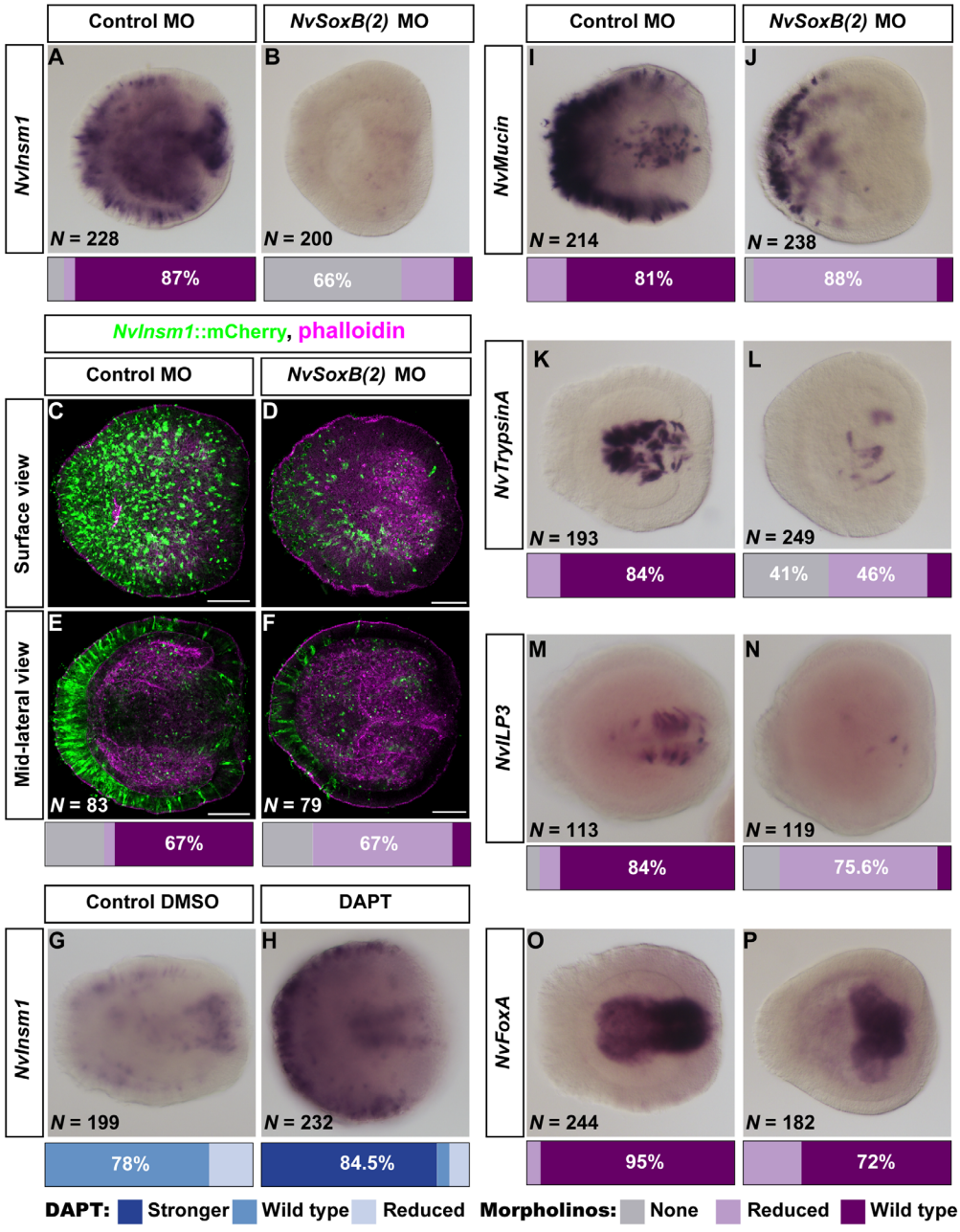


**Fig. 7. *NvSoxB(2)* is required for the development of gland/secretory cells.** (**A**, **B**, and **G** to **P**) Lateral views of ISHs at the planula stage with the aboral pole to the left. Injected morpholinos or DAPT treatment is indicated at the top, and probes are indicated on the left side. *NvSoxB(2)* MO injection results in a decreased number of *NvInsm1*- (A and B), *NvMucin*- (I and J), *NvTryspinA*- (K and L), and *NvILP3*-expressing cells (M and N). Expression of *NvFoxA* in the pharynx is present, although the shape of the pharynx is altered (O and P). (G and H) Treatment with DAPT leads to increased *NvInsm1* expression. Animals were quantified into phenotypic classes based on having no, reduced, or wild-type expression [for *NvSoxB(2)* MO injections] or based on stronger, wild-type, or reduced expression (for DAPT treatment). Bars at the bottom of each image represent the percentage of animals in each phenotypic class. *N* is the total of three biological replicates. (**C**) to (**F**) show a decrease in *NvInsm1*::mCherry$^{+}$ cells (green) after injection of the *NvSoxB(2)* MO. Phalloidin staining (magenta) allows the visualization of the morphology of the developing pharynx. Scale bars, 50 μm.

and the development of gland/secretory cells. In the *Nematostella* cell atlas (*54*), *NvNotch* and its putative ligands *NvDelta1-3* were not enriched in any of the larval metacells, but we found that *NvInsm1* is co–up-regulated with the atonal/neurogenin-related gene *NvAth-like* [and *NvSoxB(2)*] in one of the "progenitor/undifferentiated" metacells (fig. S6, A and B). *NvAshA* [a *Nematostella achaete-scute* gene; (*42*)], in contrast, was co–up-regulated with *NvInsm1* in three "neuronal" metacells, but not in progenitor/undifferentiated or gland/secretory metacells (fig. S6, A and B). This supports the notion that *NvInsm1* is mainly expressed in differentiating and/or differentiated cells. Incubation with the γ-secretase inhibitor N-[N-(3,5-difluorophenacetyl-L-alanyl)]-(S)-phenylglycine t-butyl ester (DAPT) (*58*) can be used for inhibiting Notch signaling, and it increases the number of neural cells in *Nematostella* (*43*, *45*). DAPT treatment resulted in an

increase in the number of *NvInsm1*-expressing cells in the body wall (Fig. 7, G and H), but we could not detect a clear effect on the expression of *NvMucin* in the body wall (fig. S6, G and H). The high density and strong labeling of *NvMucin*-expressing cells in the aboral part of the planula made this analysis challenging. We consistently observed a higher intensity of pharyngeal *NvILP3*, but not *NvTrypsinA* signal, in DAPT-treated animals, but we did not find evidence that the numbers of these gland/secretory cells are increased (fig. S6, C to F). DAPT-treated planulae also showed reduced expression of *NvFoxA*, suggesting a broader defect in pharynx development (fig. S6, I and J). It remains therefore unclear whether DAPT treatment has a specific effect on the development of gland/secretory cells in *Nematostella*.

Together, these observations suggest that neural and gland cells in *Nematostella* derive from a common *NvSoxB(2)*-expressing progenitor cell population and that *NvSoxB(2)* and Notch signaling are involved in the regulation of *NvInsm1* expression.

## DISCUSSION

In this study, we have shown that neurons and gland/secretory cells in *Nematostella* originate from a common population of progenitor cells that is characterized by the expression of *NvSoxB(2)*. Among the cells derived from this progenitor population, *NvInsm1* is expressed in sensory cells, ganglion cells, and gland/secretory cells. We propose a scenario in which *NvInsm1* functions at an early stage in the postmitotic differentiation program of these cells, and we interpret our findings as support for a close evolutionary relationship of neurons and gland/secretory cells.

We have previously characterized *NvSoxB(2)*-expressing cells as a population that during embryonic development includes proliferating cells (determined by EdU incorporation in pulse-labeling experiments) and that gives rise to the three classes of cnidarian neural cells: sensory cells, ganglion cells, and cnidocytes (*44*). Focusing on later developmental stages and using double transgenic animals with the brighter *NvInsm1::GFP* line, we find here that *NvSoxB(2)*$^+$ cells in addition give rise to different types of gland/secretory cells. Moreover, knockdown of *NvSoxB(2)* results in a strong reduction in the expression of genes expressed in gland/secretory cells. Inhibition of Notch signaling has been shown to increase the number of different types of neural cells in *Nematostella* (*43*, *45*, *52*), and in line with these findings, we observed an increased number of *NvInsm1*-expressing cells upon inhibition of Notch signaling via treatment with the γ-secretase inhibitor DAPT. Analyses of the effect of DAPT treatment on the number of gland/secretory cells did not reveal a similar increase, but at least for the pharyngeal cells, it is possible that the malformation of the pharynx in these animals prevented the detection of an effect on the number of these cells. The role of Notch signaling in the development of gland/secretory cells therefore remains unclear. Knockdown of *NvInsm1* reduced the expression of gland/secretory cell–specific genes, but not that of the three neural-specific genes that we analyzed here. This could mean that the expression of these genes is less sensitive to reduced levels of *NvInsm1* and that only a stronger knockdown would affect their expression. Alternatively, *NvInsm1* might function after the expression of these three genes commences and thus is not required for their regulation. We favor the former scenario since our expression analyses suggest that *NvInsm1* is expressed early during the development of neural and gland/secretory cells (see below). The clarification of the role of *NvInsm1* in neural development will benefit from a knockout allele and a more comprehensive analysis of the gene expression changes in these mutants.

While our observations show that the population of *NvSoxB(2)*-expressing cells has a broader developmental potential than previously thought [see also (*59*)], the degree of heterogeneity of progenitor cells in this population remains unknown. It might include progenitors with a developmental potential restricted to one class of cells (e.g., sensory cells or gland/secretory cells) and/or progenitors that can give rise to different classes of cells. These scenarios are not mutually exclusive, as *NvSoxB(2)* expression might be maintained while progenitors undergo divisions and experience a stepwise restriction of their developmental potential. We found that *NvInsm1* and *NvSoxB(2)* transcripts are present simultaneously in many cells during development, but there are also cells that express only one of the transcripts. In the transgenic reporter line, all *NvInsm1*::GFP-expressing cells are part of the *NvSoxB(2)*::mOrange population. Since we did not observe EdU incorporation in *NvInsm1*-expressing cells (after a 30-min pulse), this suggests that *NvInsm1* transcription commences in cells that already express *NvSoxB(2)* but do not proliferate any longer and that it is maintained after *NvSoxB(2)* transcription ceases. While *NvInsm1* is thus expressed early in postmitotic precursors of neurons and gland/secretory cells (but not in precursors of cnidocytes), it does not identify proliferating progenitors dedicated to the generation of these two large populations of cells. In adult *Hydra*, trajectory analyses of single-cell RNA sequencing data suggested a common precursor or progenitor population for neurons and gland cells (*55*), and we found here that expression of *Hydra Insm1-like* is found in neurons, in gland/secretory cells, and in their precursors. This suggests that a role for *Insm1* in the development of these cells is common to different groups of cnidarians.

On the basis of the calcium-dependent ultrafast exocytosis of their extrusive organelle, the presence of synaptic connections, and the shared developmental gene expression, cnidocytes are traditionally considered a derived neural cell type (*35*, *60*–*63*), and we were therefore surprised that *NvInsm1* is not expressed in cnidocytes. In *Hydra*, expression of *Insm1-like* has also not been detected in cnidocytes or their precursors (*55*). These observations prompt more detailed lineage tracing and functional analyses to obtain a better understanding of the developmental relationship between neurons, cnidocytes, and gland/secretory cells.

In vertebrates, *Insm1* regulates the formation of cells with secretory capacity but very different developmental origins, e.g., neurons derived from the ectoderm and intestinal endocrine cells derived from the endoderm (*23*, *26*–*28*, *64*). In *Nematostella*, neurons are generated in ectoderm and mesendoderm (*47*), whereas gland/secretory cells expressing digestive enzymes are generated in the pharyngeal ectoderm and in the septal filaments of the mesenteries, a derivative of the pharyngeal ectoderm (*48*). As in vertebrates, *NvInsm1* is thus expressed in cells in which tightly regulated secretion is thought to be of importance but which have different embryological origins. One possible explanation for this observation would be a function in the regulation of genes directly involved in the secretion process, e.g., in the biogenesis, transport, or release of secretory vesicles. This scenario is, however, not well supported by data from other model organisms. In mice, *Insm1* regulates neurogenesis in the cortex, the olfactory epithelium, and the otocyst by controlling the development of proliferative progenitors (*26*, *65*–*67*). In the

development of lung and pituitary endocrine cells, of serotonergic and adrenergic neurons, and of zebrafish motor neurons, *Insm1* instead is required for terminal differentiation (*27*, *29*, *68*, *69*), and this can include the repression of alternative differentiation programs (*29*, *70*). Despite the notable restriction of *Insm1* function to neural and endocrine cells, there are thus likely differences in the specific regulatory programs regulated by *Insm1* in different populations of cells in vertebrates. Comparisons of *Insm1* function across a broader range of animals and identification of direct target genes will likely be informative for obtaining a better understanding of the evolution of *Insm1* function.

In contrast to the *Drosophila* and *C. elegans Insm1* orthologs, *NvInsm1* encodes an N-terminal SNAG motif that in mice mediates interaction with chromatin-modifying complexes containing Lsd1/KDM1A, CoREST, and HDAC1/2 (*29*, *49*). The SNAG motif has been shown to be essential for the function of mouse Insm1 in pituitary development (*29*), and the presence of this motif in *Nematostella Insm1* might facilitate cross-species comparisons of the transcriptional regulation by Insm1 genes.

Our observations reveal developmental commonalities of cnidarian neurons and gland/secretory cells at the level of cell lineage and gene regulation. Together with previously described similarities in the development of these cell types among bilaterian species, our findings support the hypothesis that neurons and endocrine cells of extant animals evolved from primordial sensory-secretory cells (*11*, *71*–*75*).

## MATERIALS AND METHODS

### *Nematostella* culture

Animals were maintained at 18°C in one-third filtered seawater [*Nematostella* medium (NM)]. Spawning induction was performed by light and temperature shift as described in (*76*). Incubation of the fertilized egg packages with 3% cysteine/NM (pH 7.4) removed the jelly. Embryos were then raised at 21°C and fixed at 12 hours post fertilization (hpf) (early blastula), 16 hpf (blastula), 20 hpf (early gastrula), 24 hpf (gastrula), 30 hpf (late gastrula), 48 hpf (early planula), 72 hpf (planula), 4 days post fertilization (dpf) (late planula), 5 dpf (tentacle bud), and 7 dpf (primary polyp).

### Identification of *NvInsm1* and generation of transgenic lines

*NvInsm1* is derived from gene model Nve7206, retrieved from https://figshare.com/articles/Nematostella_vectensis_transcriptome_and_gene_models_v2_0/807696. The *NvInsm1*::GFP transgenic reporter line was generated by meganuclease-mediated transgenesis as described in (*77*, *78*). The genomic coordinates for the 4.6-kb regulatory region are 179.529–184.145 on scaffold 185 (http://genome.jgi.doe.gov/Nemve1/Nemve1.home.html; accessed 15 August 2019). This fragment was inserted upstream of a codon-optimized GFP via the HiFi DNA Assembly Kit [New England Biolabs (NEB) no. E5520] with the addition of a membrane-tethering CAAX domain at the C terminus to visualize the morphology of the cells expressing the reporter protein. The *NvSoxB(2)*::*mOrange* line has been described in (*44*), *NvElav1*::*mOrange* in (*47*), *NvNCol3*::*mOrange2* in (*53*), and *NvFoxQ2d*::*mOrange* in (*52*).

### ISH, EdU labeling, and immunohistochemistry

ISH and FISH were performed as described in the supplementary material in (*44*). *NvSoxB(2)* ISHs are found in figure S8 in (*79*). For combination of FISH and immunohistochemistry (IHC), FISH was performed first using the TSA Plus Cyanine 3 Kit (PerkinElmer NEL744001KT), followed by IHC with anti-GFP primary antibody (Abcam, 290) and goat anti-rabbit Alexa 488 secondary antibody (Invitrogen, A11011).

Other primary antibodies were anti-GFP (1:200; mouse, Abcam, 1218) to detect *NvInsm1*::GFP (without FISH), and anti-dsRed to detect mOrange (1:100; rabbit, Clontech, 632496). The polyclonal NvINSM1 antibody was raised by GenScript in rabbit against amino acids 3 to 170 of NvINSM1 expressed in and purified from *Escherichia coli*. The affinity-purified antibody was used at 1:100 dilution; incubation lasted for 48 hours. EdU labeling was done as 30-min, 2-hour, and 4-hour pulses followed by fixation as described in (*44*) using Click-it EdU Alexa Fluor 488 and 647 kits (Molecular Probes, C10337). For quantification, a square of 100 × 100 μm in the body column (see Fig. 1M) was analyzed after imaging by confocal microscopy.

### Microscopy and image processing

Samples were imaged either on a Nikon Eclipse E800 compound microscope with a Nikon Digital Sight DSU3 camera (for colorimetric ISHs) or on a Leica SP5 confocal microscope. For Fig. 4, samples were imaged on an Olympus FluoView FV3000 confocal microscope. Live imaging was performed on primary polyps (between 10 and 14 dpf). Polyps were live stained with Hoechst 33342 (Thermo Fisher Scientific, 62249) at 1:2000 in NM for 10 min at room temperature. Animals were then relaxed by slowly adding 1 M $MgCl_2$ and incubating the fully extended animals for 10 min. They were then mounted in this solution on a glass slide and imaged at the confocal microscope. Image manipulation was performed with Imaris (three-dimensional reconstructions of whole stacks to present embryos overviews) and with Fiji (*80*) for zoomed snapshots (single picture or stack of two to three confocal sections). Figures were assembled in Adobe Illustrator.

### Western blotting

Protein extraction was performed on wild-type late planula. Animals were placed in radioimmunoprecipitation assay buffer [150 mM NaCl, 50 mM tris (pH 8), 1% NP-40, 0.5% deoxycholate, and 0.1% SDS] supplemented with cOmplete EDTA-free protease inhibitor cocktail (Roche, 4693159001) and homogenized by passing through a 27-gauge needle. Samples were incubated on ice for 30 min and mixed by passing through the needle every 5 min and centrifuged at full speed for 15 min at 4°C. The supernatant was kept, and the protein concentration was quantified using the Qubit Protein Assay (Invitrogen, Q33212). Protein (30 μg) was used per lane, mixed 1:1 with 2× Laemmli sample buffer [0.1 M tris-HCl (pH 6.8), 2% SDS, 20% glycerol, 4% β-mercaptoethanol, and 0.02% bromophenol blue], and boiled for 5 min before loading. PageRuler Plus Prestained Protein Ladder (10 to 250 kDa; Thermo Fisher Scientific, 26619) was used. SDS–polyacrylamide gel electrophoresis was performed using 7.5% Mini-PROTEAN TGX Precast Protein Gels (Bio-Rad, 4561023) run in running buffer (25 mM tris, 192 mM glycine, and 0.1% SDS) at 100 V for ~120 min. Transfer was performed using Trans-Blot Turbo Mini 0.2 μm PVDF Transfer Pack (Bio-Rad, 1704156) on a Trans-Blot Turbo transfer system (Bio-Rad) using the high–molecular weight program. After transfer, the membrane was washed in PBT [phosphate-buffered saline (PBS) + 0.1% Tween] several times and blocked with 5% milk powder in

PBT (MPBT) at room temperature for 1 hour. The blots were incubated overnight at 4°C in primary antibody (rabbit anti-NvInsm1; concentration, 1:10,000) in MPBT. The membranes were then washed several times in PBT and incubated in secondary antibody [concentration 1:10,000; goat anti-rabbit (horseradish peroxidase), Ab97051] in MPBT at room temperature for 1 hour. Membranes were then washed several times in TBT (tris-buffered saline + 0.1% Tween), and the signal was revealed using Clarify ECL substrate (Bio-Rad, 1705060) and imaged on a ChemiDoc XRS+ (Bio-Rad).

### Morpholino injection and DAPT treatment

*NvSoxB(2)* MO and the generic control MO are described in (*44*). Experiments were conducted with three biological replicates, with embryos derived from three independent spawnings. Morpholino sequences are *NvSoxB(2)* MO1 (TATACTC TCCGCTGTGTCGCTATGT) and control MO (CCATTGTGAAGTTAAACGATAGATC). For DAPT treatment, animals were incubated in 10 μM DAPT (Sigma-Aldrich) in NM/0.1% dimethyl sulfoxide (DMSO) from cleavage stages onward. Control animals were incubated in 0.1% DMSO in NM, solutions were changed every 12 hours, and the animals were fixed at 72 hpf.

### shRNA experiments and qPCR

shRNAs were designed and synthesized as per the published protocol (*56*). Briefly, oligos were mixed to a final concentration of 20 μM, each in 20 μl, heated to 98°C for 5 min, and then allowed to cool slowly to room temperature. Solution (5.5 μl) was then used as template in a 20-μl reaction with the AmpliScribe T7 Transcription Kit (Lucigen, AS3107). Following deoxyribonuclease (DNase) treatment, the shRNA was purified using the RNA Clean and Concentrator Kit (Zymo, R1013). shRNAs were tested at a series of concentrations, and 300 ng/μl was determined to be optimum in this case. For qPCR analysis, animals were injected and allowed to develop until 72 hours; animals were lysed in 500 μl of TRIzol reagent (Invitrogen, 15596026) by vortexing extensively and incubated at room temperature for 5 min. Chloroform (100 μl) was added and mixed vigorously, and the aqueous component was isolated using MaXtract High Density tubes (QIAGEN, 129046) according to the manufacturer's protocol. One volume of 100% ethanol was added to the aqueous phase. This was then processed using the RNeasy Micro Kit (QIAGEN, 74004) according to the manufacturer's protocol including on-column DNase digestion using the RNase-Free DNase Set (QIAGEN, 79254). The SuperScript III First-Strand Synthesis System (Invitrogen, 18080051) was used to generate complementary DNA, and it was primed using random hexamers (Custom oligos, Sigma-Aldrich). qPCR was performed using the QuantiTect SYBR Green PCR Mastermix (QIAGEN, 204143) and ran on a Bio-Rad CFX96 system. Primers are listed in table S2.

### Phylogenetic analysis

Amino acid sequences (table S1) were retrieved by BLAST searches at the National Center for Biotechnology Information and via OrthoDB (www.orthodb.org/) (*81*). Zinc finger domains were determined by SMART (*82*), and only the first three zinc fingers were used for the alignment. Sequences before zinc finger 1 were removed and so were the sequences between zinc fingers 2 and 3. *Hydra*, *Trichoplax*, and *Clytia* genes with best reciprocal BLAST hits to Insm1 were omitted because they only have two zinc fingers. *Snail* sequences from *N. vectensis* and *Homo sapiens* were used as outgroup. The alignment was generated with MUSCLE 3.7 (*83*) at Phylemon 2 (http://phylemon2.bioinfo.cipf.es). The phylogenetic analysis was run with PhyML3.1 (*84*) and the WAG model at www.phylogeny.fr (*85*) with 100 bootstraps.

### Analysis of *Hydra* single-cell data

The *Hydra* single-cell analysis (*55*) gives access to the Broad Single-Cell Portal available at https://portals.broadinstitute.org/single_cell/study/SCP260/stem-cell-differentiation-trajectories-in-hydra-resolved-at-single-cell-resolution. On this portal, genes can be analyzed graphically, and each graphical picture can be saved.

## SUPPLEMENTARY MATERIALS

Supplementary material for this article is available at https://science.org/doi/10.1126/sciadv.abi7109

View/request a protocol for this paper from *Bio-protocol*.

## REFERENCES AND NOTES


1. D. Arendt, The evolutionary assembly of neuronal machinery. *Curr. Biol.* **30**, R603–R616 (2020).
2. F. Varoqueaux, D. Fasshauer, Getting nervous: An evolutionary overhaul for communication. *Annu. Rev. Genet.* **51**, 455–476 (2017).
3. P. Burkhardt, S. G. Sprecher, Evolutionary origin of synapses and neurons - Bridging the gap. *Bioessays* **39**, (2017).
4. T. Brunet, D. Arendt, From damage response to action potentials: Early evolution of neural and contractile modules in stem eukaryotes. *Philos. Trans. R. Soc. Lond. Ser. B Biol. Sci.* **371**, 20150043 (2016).
5. W. B. Kristan Jr., Early evolution of neurons. *Curr. Biol.* **26**, R949–R954 (2016).
6. B. J. Liebeskind, H. A. Hofmann, D. M. Hillis, H. H. Zakon, Evolution of Animal Neural Systems. *Annu. Rev. Ecol. Evol. Syst.* **48**, 377–398 (2017).
7. L. L. Moroz, On the independent origins of complex brains and neurons. *Brain Behav. Evol.* **74**, 177–190 (2009).
8. M. dos Reis, Y. Thawornwattana, K. Angelis, M. J. Telford, P. C. J. Donoghue, Z. Yang, Uncertainty in the timing of origin of animals and the limits of precision in molecular timescales. *Curr. Biol.* **25**, 2939–2950 (2015).
9. E. Park, D. S. Hwang, J. S. Lee, J. I. Song, T. K. Seo, Y. J. Won, Estimation of divergence times in cnidarian evolution based on mitochondrial protein-coding genes and the fossil record. *Mol. Phylogenet. Evol.* **62**, 329–345 (2012).
10. U. Ernsberger, Can the 'neuron theory' be complemented by a universal mechanism for generic neuronal differentiation. *Cell Tissue Res.* **359**, 343–384 (2015).
11. V. Hartenstein, S. Takashima, P. Hartenstein, S. Asanad, K. Asanad, bHLH proneural genes as cell fate determinants of entero-endocrine cells, an evolutionarily conserved lineage sharing a common root with sensory neurons. *Dev. Biol.* **431**, 36–47 (2017).
12. M. E. Arntfield, D. van der Kooy, β-Cell evolution: How the pancreas borrowed from the brain: The shared toolbox of genes expressed by neural and pancreatic endocrine cells may reflect their evolutionary relationship. *Bioessays* **33**, 582–587 (2011).
13. J. L. de la Pompa, A. Wakeham, K. M. Correia, E. Samper, S. Brown, R. J. Aguilera, T. Nakano, T. Honjo, T. W. Mak, J. Rossant, R. A. Conlon, Conservation of the Notch signalling pathway in mammalian neurogenesis. *Development* **124**, 1139–1148 (1997).
14. S. Lutolf, F. Radtke, M. Aguet, U. Suter, V. Taylor, Notch1 is required for neuronal and glial differentiation in the cerebellum. *Development* **129**, 373–385 (2002).
15. A. Apelqvist, H. Li, L. Sommer, P. Beatus, D. J. Anderson, T. Honjo, M. H. de Angelis, U. Lendahl, H. Edlund, Notch signalling controls pancreatic cell differentiation. *Nature* **400**, 877–881 (1999).
16. E. Cau, S. Casarosa, F. Guillemot, Mash1 and Ngn1 control distinct steps of determination and differentiation in the olfactory sensory neuron lineage. *Development* **129**, 1871–1880 (2002).
17. C. S. Lee, N. Perreault, J. E. Brestelli, K. H. Kaestner, Neurogenin 3 is essential for the proper specification of gastric enteroendocrine cells and the maintenance of gastric epithelial cell identity. *Genes Dev.* **16**, 1488–1497 (2002).
18. M. Jenny, C. Uhl, C. Roche, I. Duluc, V. Guillermin, F. Guillemot, J. Jensen, M. Kedinger, G. Gradwohl, Neurogenin3 is differentially required for endocrine cell fate specification in the intestinal and gastric epithelium. *EMBO J.* **21**, 6338–6347 (2002).
19. G. Gradwohl, A. Dierich, M. LeMeur, F. Guillemot, neurogenin3 is required for the development of the four endocrine cell lineages of the pancreas. *Proc. Natl. Acad. Sci. U.S.A.* **97**, 1607–1611 (2000).
20. M. F. Buas, T. Kadesch, Regulation of skeletal myogenesis by Notch. *Exp. Cell Res.* **316**, 3028–3033 (2010).

21. K. V. Pajcini, N. A. Speck, W. S. Pear, Notch signaling in mammalian hematopoietic stem cells. *Leukemia* **25**, 1525–1532 (2011).
22. G. Mellitzer, S. Bonné, R. F. Luco, M. van de Casteele, N. Lenne-Samuel, P. Collombat, A. Mansouri, J. Lee, M. Lan, D. Pipeleers, F. C. Nielsen, J. Ferrer, G. Gradwohl, H. Heimberg, IA1 is NGN3-dependent and essential for differentiation of the endocrine pancreas. *EMBO J.* **25**, 1344–1352 (2006).
23. M. S. Gierl, N. Karoulias, H. Wende, M. Strehle, C. Birchmeier, The zinc-finger factor Insm1 (IA-1) is essential for the development of pancreatic beta cells and intestinal endocrine cells. *Genes Dev.* **20**, 2465–2478 (2006).
24. M. B. Breslin, M. Zhu, M. S. Lan, NeuroD1/E47 regulates the E-box element of a novel zinc finger transcription factor, IA-1, in developing nervous system. *J. Biol. Chem.* **278**, 38991–38997 (2003).
25. A. Duggan, T. Madathany, S. C. P. de Castro, D. Gerrelli, K. Guddati, J. García-Añoveros, Transient expression of the conserved zinc finger gene INSM1 in progenitors and nascent neurons throughout embryonic and adult neurogenesis. *J. Comp. Neurol.* **507**, 1497–1520 (2008).
26. L. M. Farkas, C. Haffner, T. Giger, P. Khaitovich, K. Nowick, C. Birchmeier, S. Pääbo, W. B. Huttner, Insulinoma-associated 1 has a panneurogenic role and promotes the generation and expansion of basal progenitors in the developing mouse neocortex. *Neuron* **60**, 40–55 (2008).
27. J. Jacob, R. Storm, D. S. Castro, C. Milton, P. Pla, F.¸. Guillemot, C. Birchmeier, J. Briscoe, Insm1 (IA-1) is an essential component of the regulatory network that specifies monoaminergic neuronal phenotypes in the vertebrate hindbrain. *Development* **136**, 2477–2485 (2009).
28. H. Wildner, M. S. Gierl, M. Strehle, P. Pla, C. Birchmeier, Insm1 (IA-1) is a crucial component of the transcriptional network that controls differentiation of the sympatho-adrenal lineage. *Development* **135**, 473–481 (2008).
29. J. E. Welcker, L. R. Hernandez-Miranda, F. E. Paul, S. Jia, A. Ivanov, M. Selbach, C. Birchmeier, Insm1 controls development of pituitary endocrine cells and requires a SNAG domain for function and for recruitment of histone-modifying factors. *Development* **140**, 4947–4958 (2013).
30. S. Jia, H. Wildner, C. Birchmeier, Insm1 controls the differentiation of pulmonary neuroendocrine cells by repressing Hes1. *Dev. Biol.* **408**, 90–98 (2015).
31. M. J. Telford, G. E. Budd, H. Philippe, Phylogenomic Insights into Animal Evolution. *Curr. Biol.* **25**, R876–R887 (2015).
32. C. W. Dunn, G. Giribet, G. D. Edgecombe, A. Hejnol, Animal phylogeny and its evolutionary implications. *Annu. Rev. Ecol. Evol. Syst.* **45**, 371–395 (2014).
33. V. Hartenstein, A. Stollewerk, The evolution of early neurogenesis. *Dev. Cell* **32**, 390–407 (2015).
34. U. Technau, R. E. Steele, Evolutionary crossroads in developmental biology: Cnidaria. *Development* **138**, 1447–1458 (2011).
35. F. Rentzsch, M. Layden, M. Manuel, The cellular and molecular basis of cnidarian neurogenesis. *WIREs Dev. Biol.* **6**, e257 (2017).
36. B. Galliot, M. Quiquand, A two-step process in the emergence of neurogenesis. *Eur. J. Neurosci.* **34**, 847–862 (2011).
37. H. Watanabe, T. Fujisawa, T. W. Holstein, Cnidarians and the evolutionary origin of the nervous system. *Develop. Growth Differ.* **51**, 167–183 (2009).
38. T. C. Bosch, F. Anton-Erxleben, G. Hemmrich, K. Khalturin, The Hydra polyp: Nothing but an active stem cell community. *Develop. Growth Differ.* **52**, 15–25 (2010).
39. H. Watanabe, V. T. Hoang, R. Mattner, T. W. Holstein, Immortality and the base of multicellular life: Lessons from cnidarian stem cells. *Semin. Cell Dev. Biol.* **20**, 1114–1125 (2009).
40. U. Frank, G. Plickert, W. A. Muller, *Stem Cells in Marine Organisms*, B. Rinkevich, V. Matranga, Eds. (Springer, 2009), pp. 33–59.
41. M. J. Layden, F. Rentzsch, E. Röttinger, The rise of the starlet sea anemone Nematostella vectensis as a model system to investigate development and regeneration. *Wiley Interdiscip. Rev. Dev. Biol.* **5**, 408–428 (2016).
42. M. J. Layden, M. Boekhout, M. Q. Martindale, Nematostella vectensis achaete-scute homolog NvashA regulates embryonic ectodermal neurogenesis and represents an ancient component of the metazoan neural specification pathway. *Development* **139**, 1013–1022 (2012).
43. M. J. Layden, M. Q. Martindale, Non-canonical Notch signaling represents an ancestral mechanism to regulate neural differentiation. *EvoDevo* **5**, 30 (2014).
44. G. S. Richards, F. Rentzsch, Transgenic analysis of a SoxB gene reveals neural progenitor cells in the cnidarian Nematostella vectensis. *Development* **141**, 4681–4689 (2014).
45. G. S. Richards, F. Rentzsch, Regulation ofNematostellaneural progenitors by SoxB, Notch and bHLH genes. *Development* **142**, 3332–3342 (2015).
46. H. Watanabe, A. Kuhn, M. Fushiki, K. Agata, S. Özbek, T. Fujisawa, T. W. Holstein, Sequential actions of β-catenin and Bmp pattern the oral nerve net in Nematostella vectensis. *Nat. Commun.* **5**, 5536 (2014).
47. N. Nakanishi, E. Renfer, U. Technau, F. Rentzsch, Nervous systems of the sea anemone Nematostella vectensis are generated by ectoderm and endoderm and shaped by distinct mechanisms. *Development* **139**, 347–357 (2012).
48. P. R. H. Steinmetz, A. Aman, J. E. M. Kraus, U. Technau, Gut-like ectodermal tissue in a sea anemone challenges germ layer homology. *Nat. Ecol. Evol.* **1**, 1535–1542 (2017).
49. C. E. Monaghan, T. Nechiporuk, S. Jeng, S. McWeeney, J. Wang, M. G. Rosenfeld, G. Mandel, REST corepressors RCOR1 and RCOR2 and the repressor INSM1 regulate the proliferation-differentiation balance in the developing brain. *Proc. Natl. Acad. Sci. U.S.A.* **114**, E406–E415 (2017).
50. C. Stivers, T. Brody, A. Kuzin, W. F. Odenwald, Nerfin-1 and -2, novel Drosophila Zn-finger transcription factor genes expressed in the developing nervous system. *Mech. Dev.* **97**, 205–210 (2000).
51. H. Q. Marlow, M. Srivastava, D. Q. Matus, D. Rokhsar, M. Q. Martindale, Anatomy and development of the nervous system of Nematostella vectensis, an anthozoan cnidarian. *Dev. Neurobiol.* **69**, 235–254 (2009).
52. H. Busengdal, F. Rentzsch, Unipotent progenitors contribute to the generation of sensory cell types in the nervous system of the cnidarian Nematostella vectensis. *Dev. Biol.* **431**, 59–68 (2017).
53. K. Sunagar, Y. Y. Columbus-Shenkar, A. Fridrich, N. Gutkovich, R. Aharoni, Y. Moran, Cell type-specific expression profiling unravels the development and evolution of stinging cells in sea anemone. *BMC Biol.* **16**, 108 (2018).
54. A. Sebé-Pedrós, B. Saudemont, E. Chomsky, F. Plessier, M.-P. Mailhé, J. Renno, Y. Loe-Mie, A. Lifshitz, Z. Mukamel, S. Schmutz, S. Novault, P. R. H. Steinmetz, F. Spitz, A. Tanay, H. Marlow, Cnidarian cell type diversity and regulation revealed by whole-organism single-cell RNA-seq. *Cell* **173**, 1520–1534.e20 (2018).
55. S. Siebert, J. A. Farrell, J. F. Cazet, Y. Abeykoon, A. S. Primack, C. E. Schnitzler, C. E. Juliano, Stem cell differentiation trajectories inHydraresolved at single-cell resolution. *Science* **365**, eaav9314 (2019).
56. S. He, F. del Viso, C. Y. Chen, A. Ikmi, A. E. Kroesen, M. C. Gibson, An axial Hox code controls tissue segmentation and body patterning inNematostella vectensis. *Science* **361**, 1377–1380 (2018).
57. H. Marlow, E. Roettinger, M. Boekhout, M. Q. Martindale, Functional roles of Notch signaling in the cnidarian Nematostella vectensis. *Dev. Biol.* **362**, 295–308 (2012).
58. C. A. Micchelli, W. P. Esler, W. T. Kimberly, C. Jack, O. Berezovska, A. Kornilova, B. T. Hyman, N. Perrimon, M. S. Wolfe, Gamma-secretase/presenilin inhibitors for Alzheimer's disease phenocopy Notch mutations in Drosophila. *FASEB J.* **17**, 79–81 (2003).
59. A. G. Cole, S. Kaul, S. M. Jahnel, J. Steger, B. Zimmerman, R. Reischl, G. S. Richards, F. Rentzsch, P. Steinmetz, U. Technau, Muscle cell type diversification facilitated by extensive gene duplications. bioRxiv 210658 (2020).
60. I. A. Westfall, Ultrastructure of synapses in the first-evolved nervous systems. *J. Neurocytol.* **25**, 735–746 (1996).
61. D. Oliver, M. Brinkmann, T. Sieger, U. Thurm, Hydrozoan nematocytes send and receive synaptic signals induced by mechano-chemical stimuli. *J. Exp. Biol.* **211**, 2876–2888 (2008).
62. T. Nuchter, M. Benoit, U. Engel, S. Ozbek, T. W. Holstein, Nanosecond-scale kinetics of nematocyst discharge. *Curr. Biol.* **16**, R316–R318 (2006).
63. B. Galliot, M. Quiquand, L. Ghila, R. de Rosa, M. Miljkovic-Licina, S. Chera, Origins of neurogenesis, a cnidarian view. *Dev. Biol.* **332**, 2–24 (2009).
64. L. D. Horb, Z. H. Jarkji, M. E. Horb, Xenopus insm1 is essential for gastrointestinal and pancreatic endocrine cell development. *Dev. Dyn.* **238**, 2505–2510 (2009).
65. S. M. Lorenzen, A. Duggan, A. B. Osipovich, M. A. Magnuson, J. Garcia-Anoveros, Insm1 promotes neurogenic proliferation in delaminated otic progenitors. *Mech. Dev.* **138** Pt 3, 233–245 (2015).
66. S. Tavano, E. Taverna, N. Kalebic, C. Haffner, T. Namba, A. Dahl, M. Wilsch-Bräuninger, J. T. M. L. Paridaen, W. B. Huttner, Insm1 induces neural progenitor delamination in developing neocortex via downregulation of the adherens junction belt-specific protein plekha7. *Neuron* **97**, 1299–1314.e8 (2018).
67. J. N. Rosenbaum, A. Duggan, J. Garcia-Anoveros, Insm1 promotes the transition of olfactory progenitors from apical and proliferative to basal, terminally dividing and neuronogenic. *Neural Dev.* **6**, 6 (2011).
68. S. Jia, A. Ivanov, D. Blasevic, T. Müller, B. Purfürst, W. Sun, W. Chen, M. N. Poy, N. Rajewsky, C. Birchmeier, Insm1 cooperates withNeurod1 andFoxa2 to maintain mature pancreatic β-cell function. *EMBO J.* **34**, 1417–1433 (2015).
69. J. Gong, X. Wang, C. Zhu, X. Dong, Q. Zhang, X. Wang, X. Duan, F. Qian, Y. Shi, Y. Gao, Q. Zhao, R. Chai, D. Liu, Insm1a regulates motor neuron development in zebrafish. *Front. Mol. Neurosci.* **10**, 274 (2017).
70. T. Wiwatpanit, S. M. Lorenzen, J. A. Cantú, C. Z. Foo, A. K. Hogan, F. Márquez, J. C. Clancy, M. J. Schipma, M. A. Cheatham, A. Duggan, J. García-Añoveros, Trans-differentiation of outer hair cells into inner hair cells in the absence of INSM1. *Nature* **563**, 691–695 (2018).
71. G. Jekely, The chemical brain hypothesis for the origin of nervous systems. *Philos. Trans. R. Soc. Lond. Ser. B Biol. Sci.* **376**, 20190761 (2021).
72. H. Grundfest, *Essays on Physiological Evolution*, J. W. S. Pringle, Ed. (Pergamon Press, 1965), pp. 107–138.
73. T. L. Lentz, Primitive nervous systems, in *The Evolutionary Origin of the Nervous System* (Yale Univ. Press, 1968).

74. H. Grundfest, *Evolution of Nervous Control from Primitive Organisms to Man*, A. D. Bass, Ed. (American Association for the Advancement of Science, 1959), vol. 52, pp. 43–87.
75. L. L. Moroz, Multiple Origins of Neurons From Secretory Cells. *Front. Cell Dev. Biol.* **9**, 669087 (2021).
76. J. H. Fritzenwanker, U. Technau, Induction of gametogenesis in the basal cnidarian Nematostella vectensis(Anthozoa). *Dev. Genes Evol.* **212**, 99–103 (2002).
77. E. Renfer, A. Amon-Hassenzahl, P. R. Steinmetz, U. Technau, A muscle-specific transgenic reporter line of the sea anemone, Nematostella vectensis. *Proc. Natl. Acad. Sci. U.S.A.* **107**, 104–108 (2010).
78. E. Renfer, U. Technau, Meganuclease-assisted generation of stable transgenics in the sea anemone Nematostella vectensis. *Nat. Protoc.* **12**, 1844–1854 (2017).
79. O. Tournière, D. Dolan, G. S. Richards, K. Sunagar, Y. Y. Columbus-Shenkar, Y. Moran, F. Rentzsch, NvPOU4/Brain3 functions as a terminal selector gene in the nervous system of the cnidarian nematostella vectensis. *Cell Rep.* **30**, 4473–4489.e5 (2020).
80. J. Schindelin, I. Arganda-Carreras, E. Frise, V. Kaynig, M. Longair, T. Pietzsch, S. Preibisch, C. Rueden, S. Saalfeld, B. Schmid, J. Y. Tinevez, D. J. White, V. Hartenstein, K. Eliceiri, P. Tomancak, A. Cardona, Fiji: An open-source platform for biological-image analysis. *Nat. Methods* **9**, 676–682 (2012).
81. E. V. Kriventseva, D. Kuznetsov, F. Tegenfeldt, M. Manni, R. Dias, F. A. Simão, E. M. Zdobnov, OrthoDB v10: Sampling the diversity of animal, plant, fungal, protist, bacterial and viral genomes for evolutionary and functional annotations of orthologs. *Nucleic Acids Res.* **47**, D807–D811 (2019).
82. I. Letunic, S. Khedkar, P. Bork, SMART: Recent updates, new developments and status in 2020. *Nucleic Acids Res.* **49**, D458–D460 (2021).
83. R. C. Edgar, MUSCLE: Multiple sequence alignment with high accuracy and high throughput. *Nucleic Acids Res.* **32**, 1792–1797 (2004).
84. S. Guindon, O. Gascuel, A simple, fast, and accurate algorithm to estimate large phylogenies by maximum likelihood. *Syst. Biol.* **52**, 696–704 (2003).
85. A. Dereeper, V. Guignon, G. Blanc, S. Audic, S. Buffet, F. Chevenet, J.-F. Dufayard, S. Guindon, V. Lefort, M. Lescot, J.-M. Claverie, O. Gascuel, Phylogeny.fr: Robust phylogenetic analysis for the non-specialist. *Nucleic Acids Res.* **36**, W465–W469 (2008).

**Acknowledgments:** We thank E. Myrvold and L. Jubek for excellent care of the *Nematostella* facility, P. Burkhardt and T. Hoffmeyer for sharing reagents and providing advice on Western blotting, J. Kraus for advice on live imaging, M. Chatzigeorgiou for helpful discussions and advice, and E. Gilbert and G. Richards for help with initial experiments. **Funding:** The work was funded by the Sars Centre Core budget and by a grant from the Research Council of Norway and the University of Bergen (251185/F20) to F.R. **Author contributions:** O.T. performed and analyzed all experiments except those shown in Fig. 4 and fig. S2J, designed the experiments, contributed to the conceptualization, generated the figures, wrote the first draft together with F.R., and edited the manuscript. H.B. performed and analyzed the experimental work shown in Fig. 4 (A to D), performed and analyzed some of the experiments shown in Fig. 7, and commented on the manuscript. J.M.G. performed and analyzed the experiments shown in Figs. 5 (A to D) and 7 (G, H, O, and P) and figs. S2J and fig. S6 (C to J) and commented on the manuscript. N.B. performed and analyzed the ISHs in Fig. 5 (E to L). F.R. conceptualized and supervised the study, wrote the first draft together with O.T., and edited the manuscript. **Competing interests:** The authors declare that they have no competing interests. **Data and materials availability:** All data needed to evaluate the conclusions in the paper are present in the paper and/or the Supplementary Materials. Transgenic animals described in this study can be provided pending a completed material transfer agreement. Requests for plasmids and transgenic lines should be submitted to F.R.

Submitted 15 April 2021
Accepted 2 March 2022
Published 20 April 2022
10.1126/sciadv.abi7109

ScienceAdvances

# *Insm1*-expressing neurons and secretory cells develop from a common pool of progenitors in the sea anemone *Nematostella vectensis*

Océane TournièreJames M. GahanHenriette BusengdalNatascha BartschFabian Rentzsch

*Sci. Adv.*, 8 (16), eabi7109. • DOI: 10.1126/sciadv.abi7109



*Science Advances* (ISSN ) is published by the American Association for the Advancement of Science. 1200 New York Avenue NW, Washington, DC 20005. The title *Science Advances* is a registered trademark of AAAS.